

# The Analysis of Underexpanded Jet Flows for Hypersonic Aerodynamic Experiments in Vacuum Chambers

V.V. Riabov<sup>1</sup> and A.I. Fedoseyev<sup>2</sup>

## 1 Introduction

Underexpanded jets have become widely used in studies of rarefied-gas flows [1]-[3] and aerodynamics of hypersonic probes in wind tunnels [4]-[7]. The objective of the present study is to analyze shapes and flow parameters in internal regions of hypersonic underexpanded viscous jets, and to apply the jet theory to hypersonic studies. Analytical solutions [7] are used for estimating internal flow parameters. The role of kinetic effects in the expanding flows of Ar and He is evaluated using the direct simulation Monte-Carlo (DSMC) technique [8]. Rotational relaxation is analyzed using quantum concepts [9], [10]. Aerodynamic characteristics of wedges, disks, and plates are studied in experiments with hypersonic underexpanded jets of He, Ar,  $N_2$ , and  $CO_2$ , and compared with the DSMC calculations [11]. Similarity parameters and fundamental aerodynamics laws are discussed.

## 2 The Shape and Properties of Underexpanded Jets

The structure of supersonic inviscid gas jets discharged from an underexpanded nozzle at  $p_j \gg p_a$  (where  $p_j$  is the pressure at the nozzle exit and  $p_a$  is the outside pressure) was analyzed in [1]-[3], [12] in detail. It was found that a considerable part of the hypersonic flow inside the jet bounded by shock waves (where  $p < p_a$ ) becomes significantly overexpanded relative to the outside pressure. The overexpansion has a maximum value. If Mach number  $M_j = 1$  at the jet exit, this value is determined by the axial location of the "Mach disk"  $x_d = 1.34r_j(p_0/p_a)^{0.5}$  [1]. The coefficient (1.34) is not sensitive to the type of perfect gas [13]. The overexpansion phenomenon inside the hypersonic underexpanded jet is important for experiments

---

<sup>1</sup>Rivier University, 420 S. Main St., Nashua, NH 03060, USA

<sup>2</sup>CFDRC, 215 Wynn Dr., Huntsville, AL 35805, USA

in vacuum chambers, where the pressure restoration occurs automatically, without the use of a diffuser [4]-[7].

Following [12], consider the steady expansion of a jet from an orifice of radius  $r_j$  in the polar coordinates  $(r, \varphi)$  with the origin at the jet exit. At large distances  $r \gg r_j$  from the nozzle exit the isentropic flow in a jet asymptotically approaches, along the ray  $\varphi = \text{const}$ , the flow from a spherical source (of radius  $R_j^o(\varphi)$ ) having an intensity which varies from ray to ray [14]. For a hypersonic inviscid gas flow the asymptotic solution for Mach number  $M$  along the ray was found in [7], [12].

The values of function  $R_j^o(\varphi)$  were found using the method of characteristics [12] and approximated by the formula  $R_j^o(\varphi) = R_j^o(0) \cos(0.5\pi\varphi/\Phi)$  that was obtained [1] by approximating the relation for the density. The values  $R_j^o(0)$  and  $\Phi$  are determined by  $\gamma$  [3], [12]. For  $\gamma = 5/3; 1.4; 9/7$ , the values for  $R_j^o(0) = 1.35; 1.15; 1.08$ ; and  $\Phi = 1.365; 1.662; 1.888$ , correspondingly.

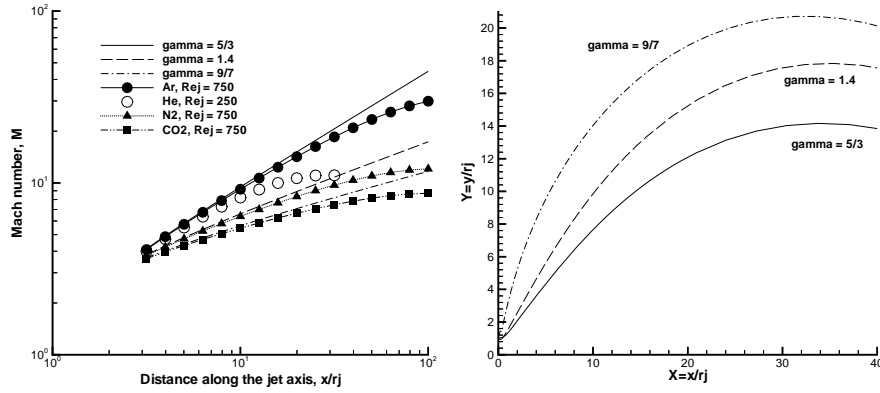


**Fig. 1** *Left*: Mach number along the axis of axisymmetric jets of Ar, He, N<sub>2</sub> and CO<sub>2</sub>. *Right*: Barrel shocks of inviscid axisymmetric jets for various gases at pressure ratio  $p_0/p_a = 1000$

The result of calculations of  $M$  along the jet axis ( $\varphi = 0$ ) is presented in Fig. 1 (*left*) for gases with different values of  $\gamma$ . When the flow within the jet is overexpanded relative to the external pressure ( $p < p_a$ ), a barrel shock with a compression layer adjacent to it develops in the jet. In the case of an axisymmetric jet expanding from a sonic orifice, the method of solving this problem was offered in [12]. Following this technique (with minor corrections), the shock shapes were calculated for gases with different parameters  $\gamma$  and  $p_0/p_a$ . The results of calculations for  $M_j = 1$ ,  $p_0/p_a = 1000$ , and  $\gamma = 5/3, 1.4$ , and  $9/7$  are shown in Fig. 1 (*right*).

The dimensions  $(x_m, y_m)$  of the jet expanded from a nozzle are shown in Fig. 2. They indicate the maximum distance of the compression shock from the jet axis as a function of  $p_0/p_a$ . The numerical results (curves) correlate well with the experimental data from [12] ( $\gamma = 5/3$ , open circles) and [15] ( $\gamma = 5/3$ , filled circles;  $\gamma = 1.4$ , triangles).

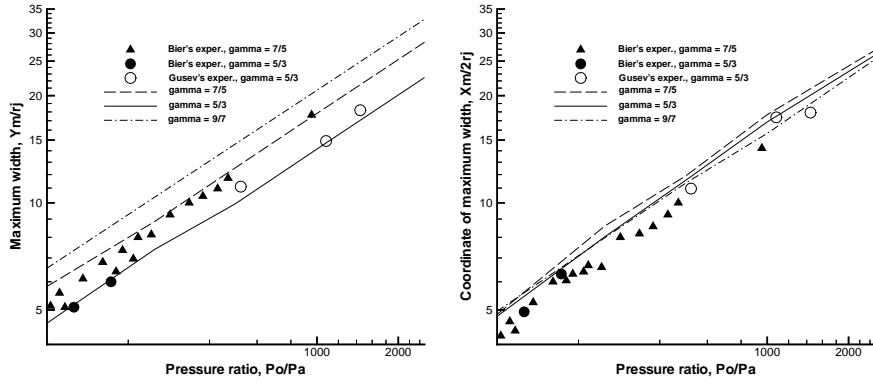


**Fig. 2** *Left*: The maximum width  $Y_m = y_m/r_j$  of inviscid axisymmetric jets ( $M_j = 1$ ) for gases with different  $\gamma$  and at various pressure ratios  $p_0/p_a$ . *Right*: The axis coordinate  $x_m$  of the width  $y_m$

The analysis of viscous effects in jets was performed in [3]-[7], [14]. It was shown that at distances  $r/r_j = O(Re_j^\omega)$ ,  $\omega = 1/[2\gamma - 1 - 2(\gamma - 1)n]$ , from the source in the flow, dissipative processes become important. The results of calculations of Mach number  $M$  along the axis of the axisymmetric viscous jet are presented in Fig. 1 (*left*) for Ar, He,  $N_2$ , and  $CO_2$  at  $T_0 = 295$  K and various  $Re_j$ .

Kinetic effects in the spherical expanding flows of Ar and He were studied using the DSMC method [8] at Knudsen numbers  $Kn_*$  from 0.0015 to 0.015 (or Reynolds numbers  $Re_*$  from 1240 to 124). The effect of freezing the parallel temperature  $T_{tx}$  was analyzed. The point of a gradual rise of  $T_{tx}$  above the continuum value is associated with the breakdown of continuum flow in expansions [8]. The transverse temperature  $T_{ty}$  follows the temperature in the isentropic expansion.

The studies on rotational (R-T) relaxation in the expansion of a molecular gas into vacuum were reviewed in [9]. A sharp drop in the gas density downstream leads to a decrease in the number of molecular collisions, and the departure of the rotational energy from the equilibrium value is observed. Another cause for the departure could be explained in terms of quantum concepts [10]. Because of the sharp decrease in  $T_t$  (below 100 K for  $N_2$ ), the highly excited rotational levels become unable to relax, and the relaxation time increases. The experimental data [16] and computations [10] demonstrate the necessity of a consideration of the quantum concept in describing R-T relaxation in free jets.

### 3 Aerodynamic Similarity Criteria and Test Results

The Reynolds number  $Re_0$ , in which the viscosity coefficient is calculated by means of stagnation temperature  $T_0$  estimated at "frozen" upstream conditions, can be con-

sidered as the main similarity parameter for modeling hypersonic flows in continuum, transitional and free-molecular regimes [4]. Using  $Re_0$  and other similarity parameters ( $\gamma$ ,  $M_\infty$ ), it is possible to perform other well-known parameters, such as the parameter  $\chi$  for pressure approximation and the parameter  $V$  for skin-friction approximation [7]:  $\chi = M_\infty^2/[0.5(\gamma-1)Re_0]^{0.5}$  and  $V = 1/[0.5(\gamma-1)Re_0]^{0.5}$ .  $Re_0$  also scales the flow rarefaction, which is characterized by the Knudsen number  $Kn_{\infty,L}$  [4], [11]. The  $Re_0$  values can be changed by relocation of a probe along the jet axis at different distances  $x$  from a nozzle exit ( $Re_0 \sim x^{-2}$ ). Due to this method, fundamental laws of hypersonic streamlining of bodies were discovered and valuable experimental data on aerothermodynamics of various probes was collected [4]-[7].

The role of other similarity parameters ( $\gamma$  and temperature factor  $t_w$ ) is studied here. The testing was performed in jets of He, Ar,  $N_2$ , and  $CO_2$  in a vacuum wind tunnel [5]-[7] at  $T_0 = 295$  K and 950 K. Plates, wedges, and disks were selected as probes. The presence of a nonuniform field in the expanding flow and experimental errors (5-8 percent) were evaluated by techniques described in [5]-[7]. The length of the model was chosen as specific linear measure, and the planform area were selected for the calculation of aerodynamic coefficients ( $c_x$ ,  $c_y$ ) and  $Re_0$ .

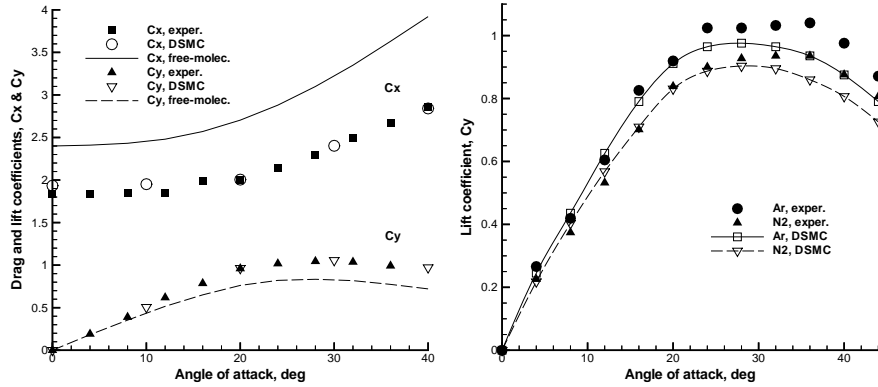


**Fig. 3** *Left*: Drag and lift coefficients  $c_x$ ,  $c_y$  for a wedge ( $2\theta = 40$  deg) in He at  $Re_0 = 4$  and  $M_\infty = 11.8$ . *Right*: Lift coefficient  $c_y$  of the wedge at  $Re_0 = 3$  in Ar and  $N_2$

The dependency of drag and lift coefficients  $c_x$  and  $c_y$  of the wedge ( $2\theta = 40$  deg) on the angle of attack was examined in He at  $Re_0 = 4$  ( $Kn_{\infty,L} = 0.3$ ),  $t_w = 1$ , and  $M_\infty = 11.8$ . The comparison of the testing data with DSMC results [11] is shown in Fig. 3 (*left*). The results indicate the advantages of the probe flight at transitional conditions in comparison with the free-molecular data (curves) [17]. The lift in the transitional regime is bigger than the free-molecular lift by a factor of 1.25.

In the free-molecular regime [17], aerodynamic characteristics of bodies depend on the normal component of the momentum of the reflected molecules, which depends on  $\gamma$ . The drag of thin bodies is proportionate to  $(\gamma + 1)$  at the regime of

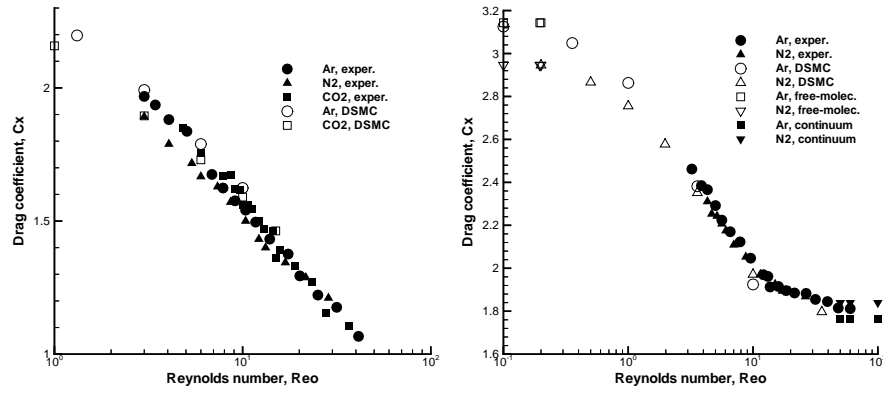


**Fig. 4** Drag coefficient  $c_x$  for a wedge ( $2\theta = 40$  deg) *left* and for a disc at  $\alpha = 90$  deg *right* for various gases vs. the Reynolds number  $Re_0$ . DSMC data from [11]

hypersonic stabilization [6]. The same conclusion is derived from tests conducted with Ar,  $N_2$ , and  $CO_2$ . The dependencies of  $c_x$  of the wedge ( $2\theta = 40$  deg) are shown in Fig. 4 (*left*) at various  $Re_0$  and  $\gamma$ . Testing data are compared with the DSMC data [6], [11]. At  $Re_0 \rightarrow 0$ , a small increase of  $c_x$  is observed as  $\gamma$  grows. Identical dependency was found in the testing for transitional regime at  $Re_0 \leq 10$  (5 percent). As the number  $Re_0$  increases, this influence decreases.

This phenomenon takes place in the case of streamlining of the wedge ( $2\theta = 40$  deg) at  $0 < \alpha \leq 40$  deg and  $Re_0 = 3$ . The experimental data for Ar and  $N_2$  and the DSMC results [11] are shown in Fig. 3 (*right*). The correlation of the data for different  $\gamma$  demonstrates a significant difference (10 percent) in the values of  $c_y$ .

The dependencies of  $c_x$  of the disc in Ar and  $N_2$  are shown in Fig. 4 (*right*) for a wide range of  $Re_0$ . The experimental data obtained for Ar and  $N_2$  are compared with DSMC data [11] and their limits in free-molecular and continuum regimes, which demonstrate different signs of  $\gamma$ -influences in the regimes.

Compared to other similarity parameters, the temperature factor ( $t_w = T_w/T_0$ ) is the most important one [4]-[7]. As an example, experimental data for  $c_x$  and  $c_y$  of a blunt plate ( $\delta = 0.1$ ) is shown in Fig. 5 for wide range of  $Re_0$ . The lift changes non-monotonically from continuum to free-molecular flow regime. Maximum values occur in the transitional flow regime. The influence of  $t_w$  can be estimated as 35 percent for the lift-drag ratio. The DSMC results [11] correlate well with the experimental data at  $Re_0 \leq 10$ . Decreasing  $t_w$  decreases the pressure at the body surface in comparison with the tangential stresses [6], [7]. Therefore,  $c_y$  is the most sensitive parameter to changes of  $t_w$  in the transitional flow regime (see Fig. 5, *right*).

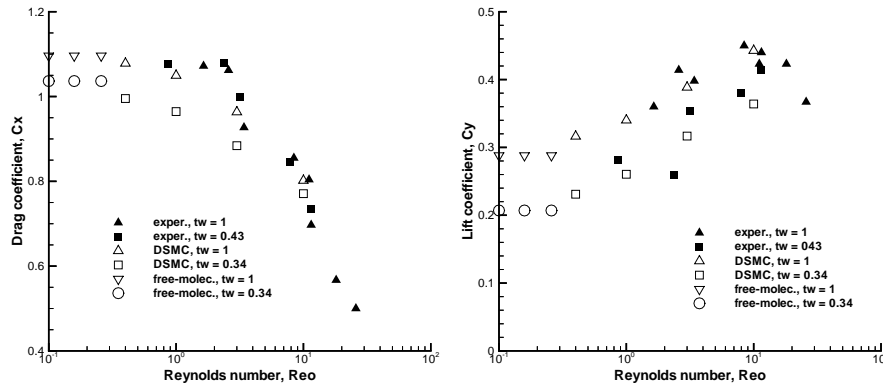


**Fig. 5** Drag (*left*) and lift (*right*) coefficients  $c_x$ ,  $c_y$  for the blunt plate ( $\delta = 0.1$ ) vs. Reynolds number  $Re_0$  in nitrogen at  $\alpha = 20$  deg and various temperature factors  $t_w$ . DSMC data from [11]

## 4 Concluding Remarks

Methods used in this study allow the user to explore effectively hypersonic gas flows in the underexpanded jets and test probes in the transitional regime between free-molecular and continuum regimes. Good correlation is noticed between testing data and DSMC numerical results. The acquired information could be effectively used for prediction of aerodynamic characteristics of hypersonic vehicles at low-density flight conditions in atmospheres of the Earth, Mars, Venus, and other planets.

## References

1. Ashkenas, H., Sherman, F.S.: 4th RGD Symp. **2**, 84-105 (1965)
2. Muntz, E.P., Hamel, B.B., Maguire, B.L.: AIAA J. **8**(9) (1970)
3. Rebrov, A.K.: J. Vac. Sci. Technol. A **19**(4) (2001)
4. Gusev, V.N., Kogan, M.N., Perepukhov, V.A.: Uch. Zap. TsAGI **1**(1) (1970)
5. Gusev, V.N., Klimova, T.V., Riabov, V.V.: Uch. Zap. TsAGI **7**(3) (1976)
6. Gusev, V.N., et al.: Trudy TsAGI **1855**, 1-43 (1977)
7. Riabov, V.V.: J. Aircraft **32**(3) (1995)
8. Riabov, V.V.: J. Thermophys. Heat Tr. **17**(4) (2003)
9. Riabov, V.V.: J. Thermophys. Heat Tr. **14**(3) (2000)
10. Lebed, I.V., Riabov, V.V.: J. Appl. Mech. Tech. Phys. **20**(1) (1979)
11. Riabov, V.V.: J. Spacecr. Rockets **35**(4) (1998)
12. Gusev, V.N., Klimova, T.V.: Fluid Dyn. **3**(4) (1968)
13. Crist, S., Sherman, P.M., Glass, D.R.: AIAA J. **4**(1) (1966)
14. Gusev, V.N., Klimova, T.V., Riabov, V.V.: Fluid Dyn. **13**(6) (1978)
15. Bier, K., Schmidt, B.: Z. Angew. Phys. **13**(11) (1961)
16. Borzenko, B.N., Karelov, N.V., Rebrov, A.K., et al.: J. Appl. Mech. Tech. Phys. **17**(5) (1976)
17. Kogan, M.N.: Rarefied Gas Dynamics, Plenum Press: New York (1969)